FCC-EE MDI
ALIGNMENT SYSTEM UPDATE

Reminder of the FCC-ee MDI region

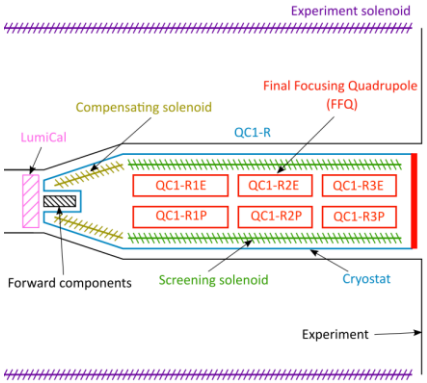

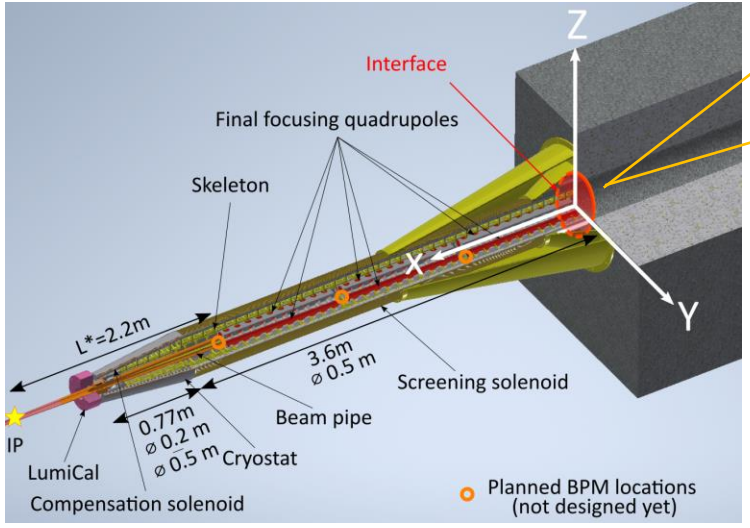

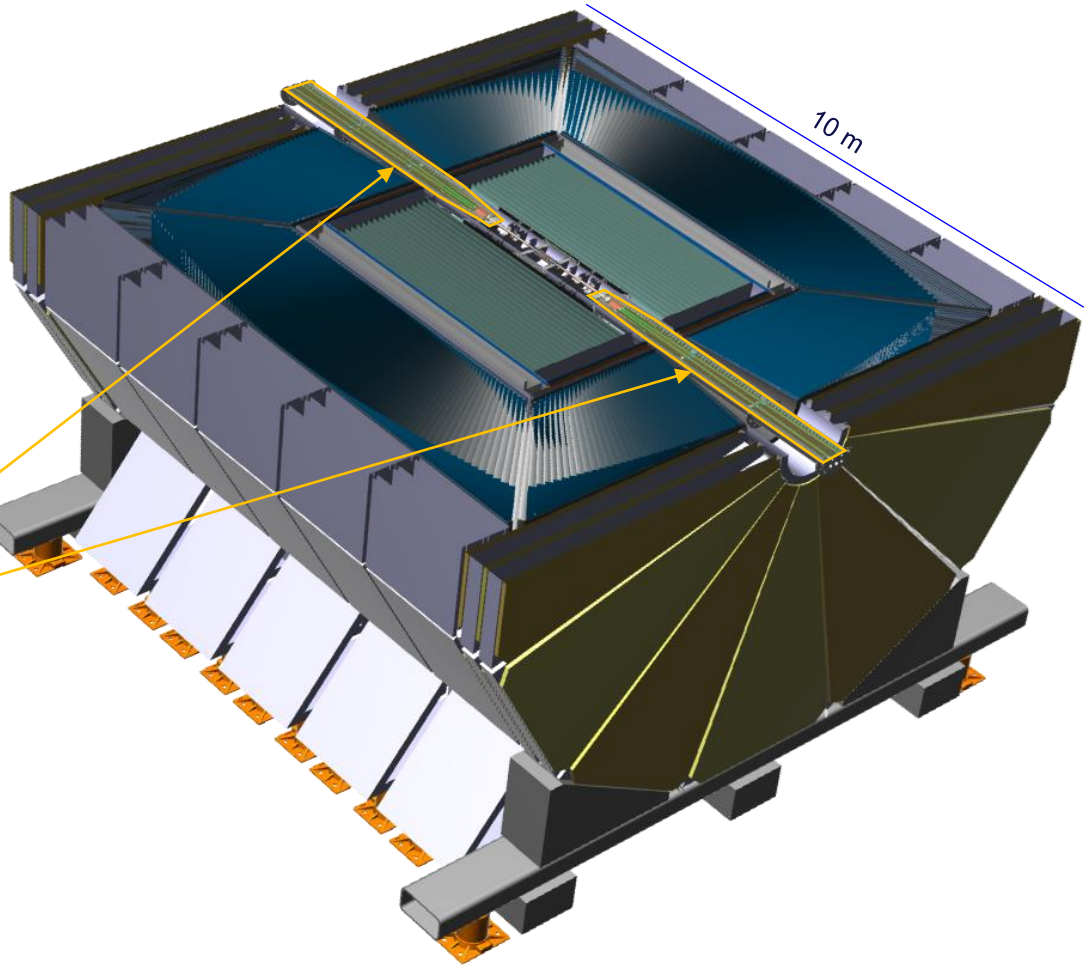

The access challenge

Only access available

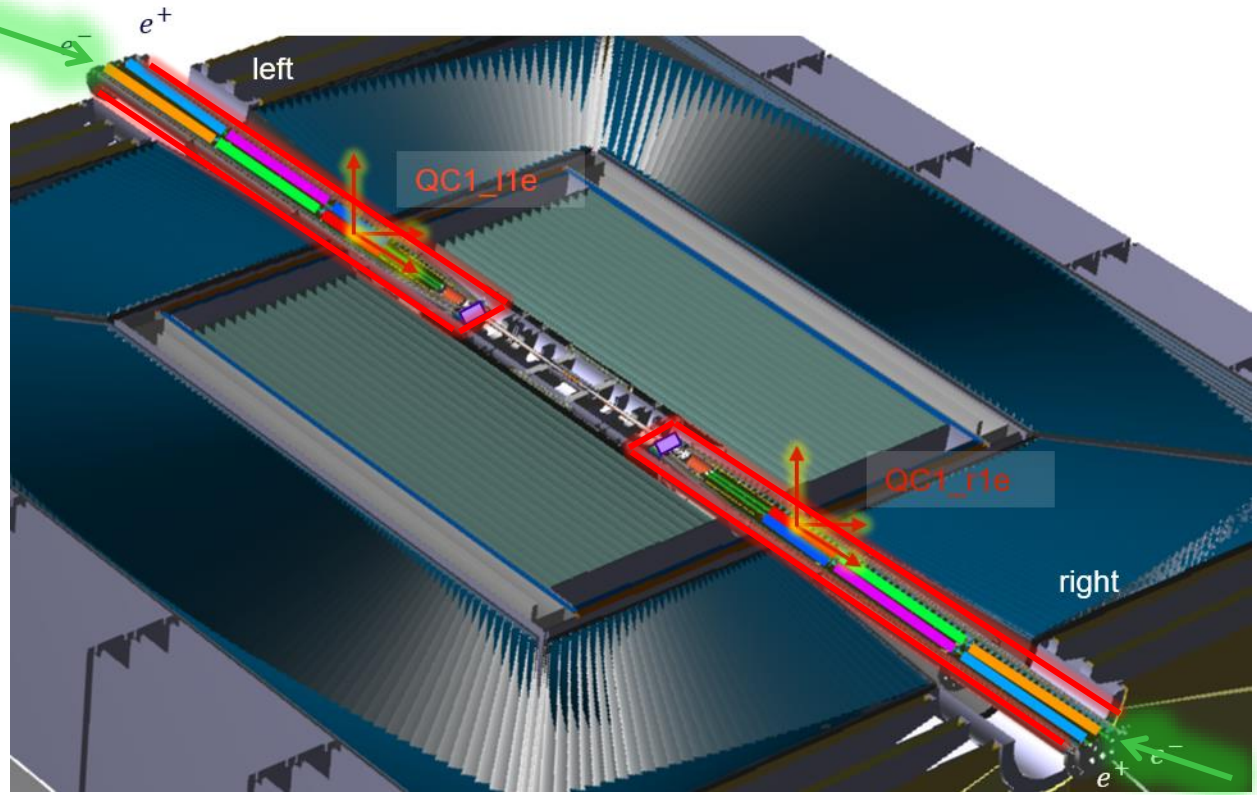

Only access available

Reaching the end of the assembly from the extremity thanks to optical fibers

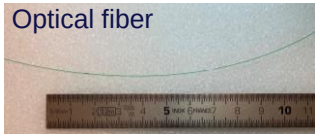

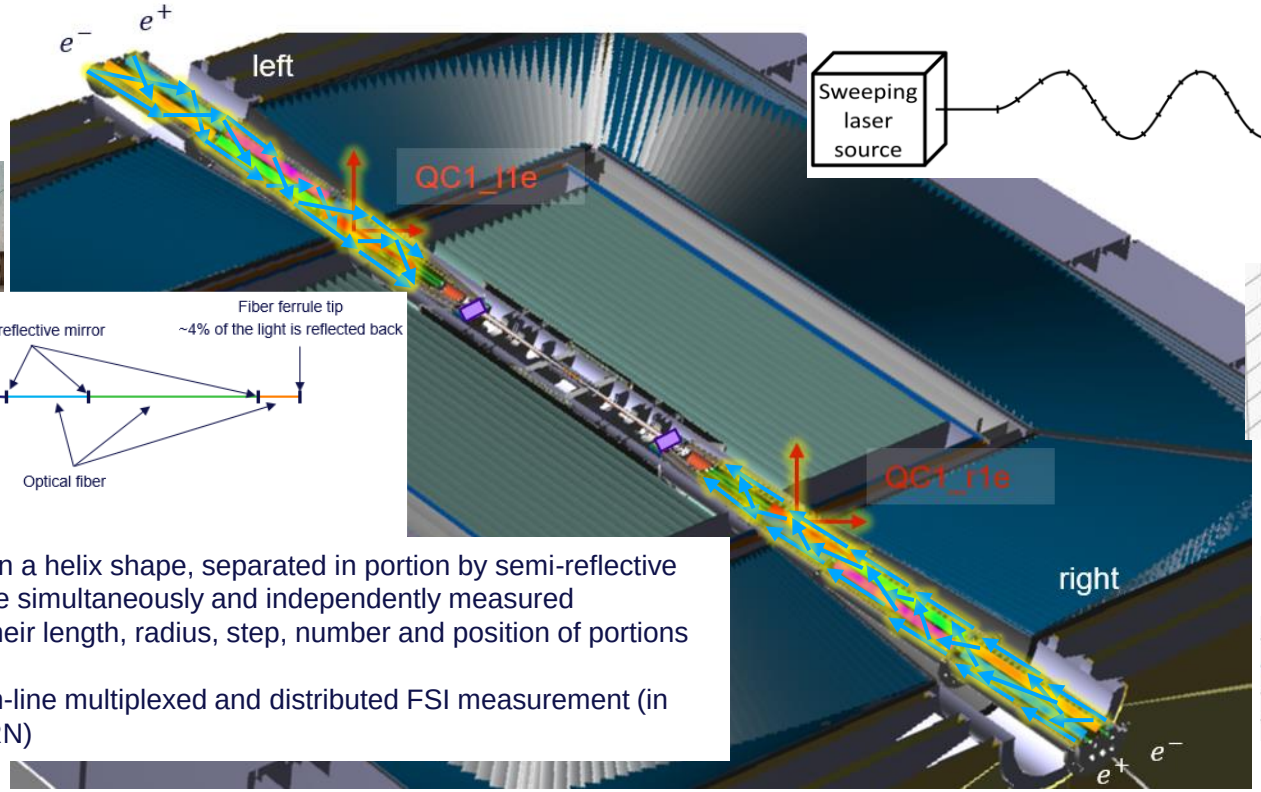

- Optical fiber placed in a helix shape, separated in portion by semi-reflective mirrors, which can be simultaneously and independently measured
- Helixes defined by their length, radius, step, number and position of portions

- Technology used : In-line multiplexed and distributed FSI measurement (in development at CERN)

Impact of deformation on a singular fiber

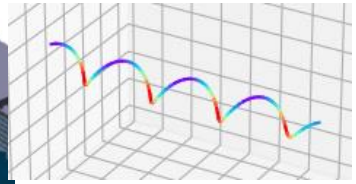

Impact of deformation on a network of fibers

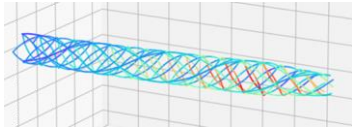

https://iopscience.iop.org/article/10.1088/1361-6501/acc6e3

Establishing a reference to measure the final focusing quadrupoles

Fiber optic helix network deformation simulations

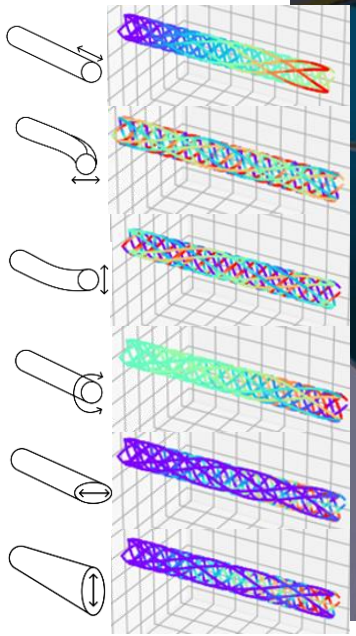

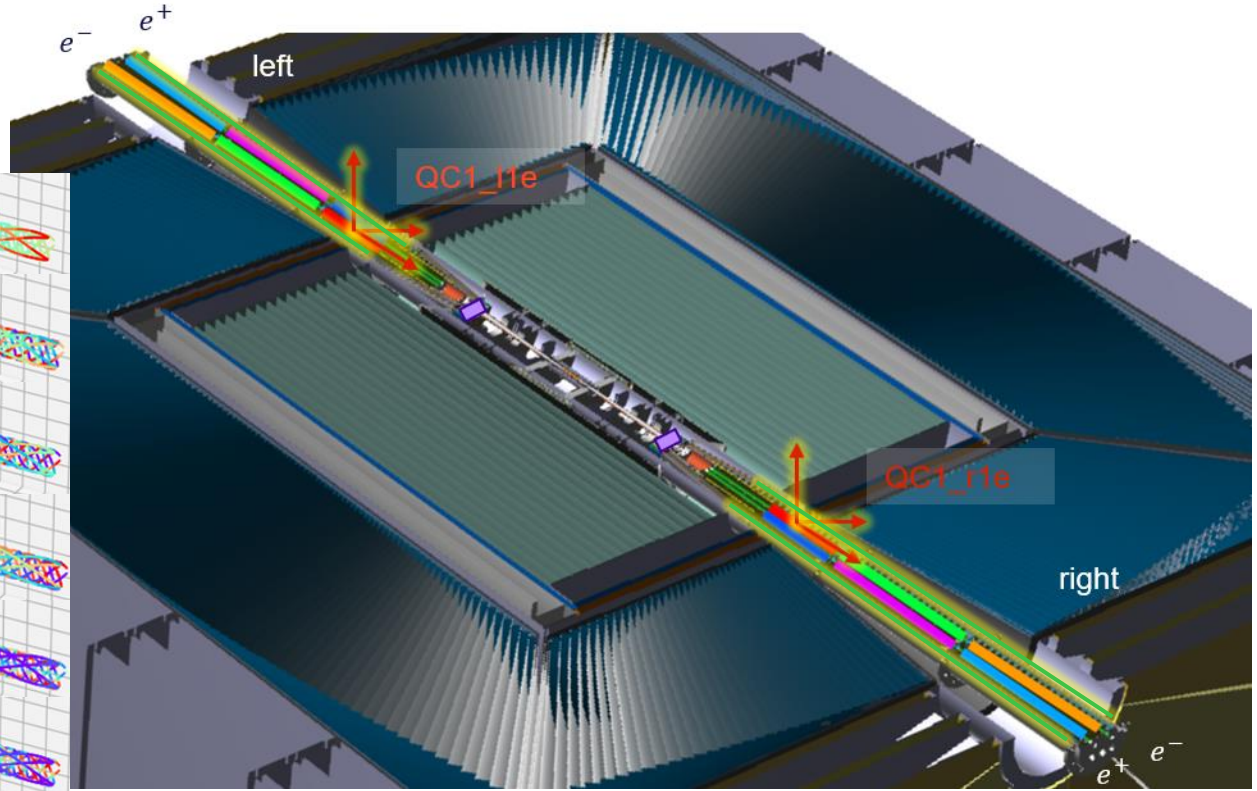

Least square computation of the deformation from the measurements

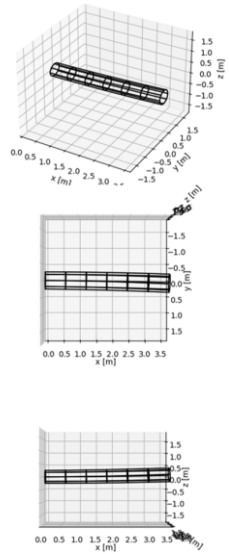

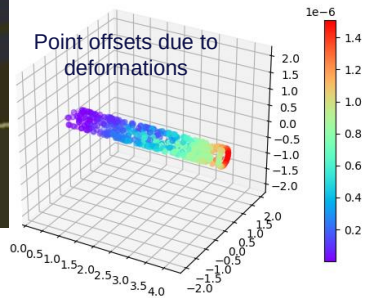

https://iopscience.iop.org/article/10.1088/1361-6501/acc6e3

Measurement of the final focusing quadrupoles

Laser emitting ferrule

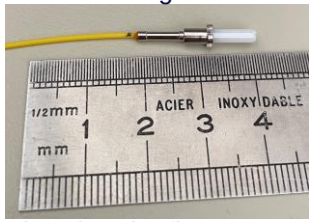

Glass bead reflectors

Prototype

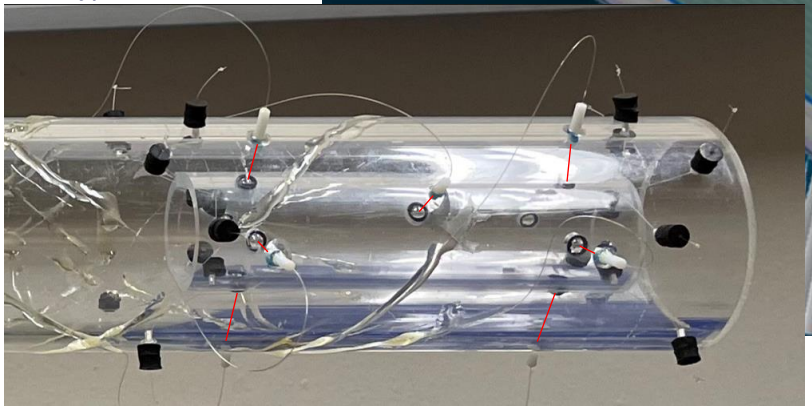

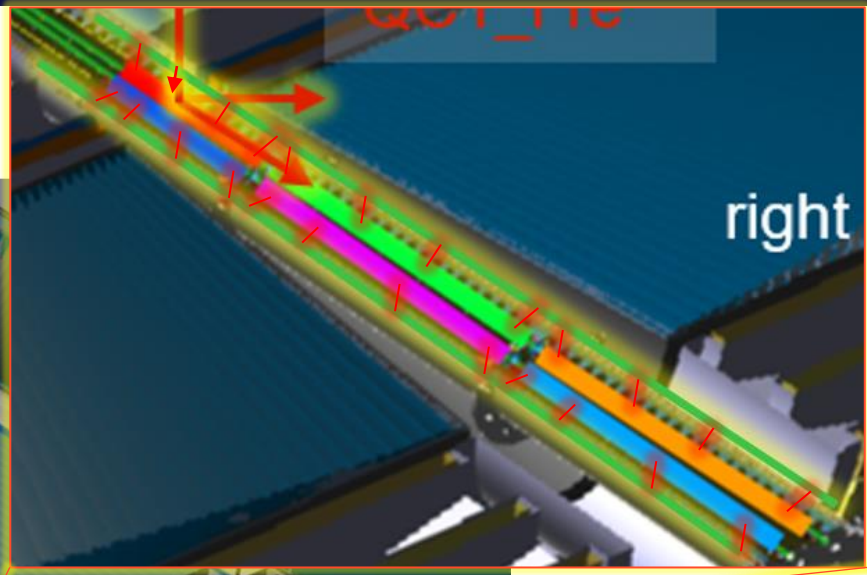

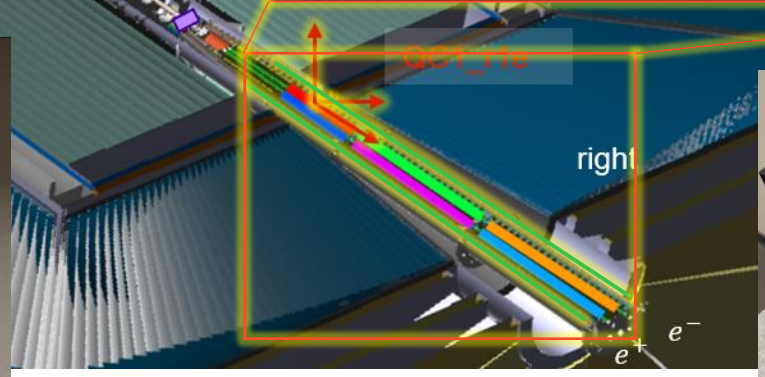

Prism for compact laser delivery

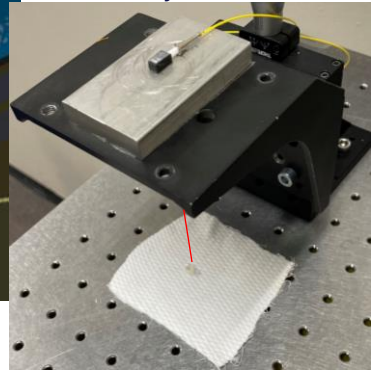

Article link

Latest and ongoing prototypes

First prototype with helix fibers

Monitoring of the glue curing

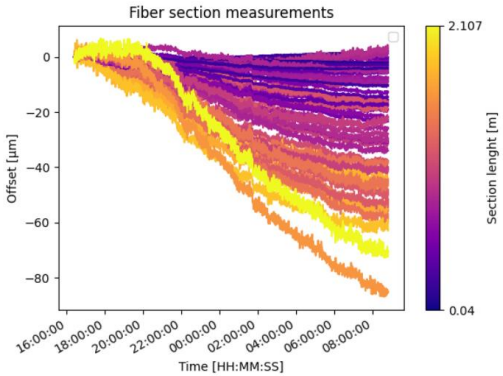

Article link

Prototype implementing the fiber measurement and the FSI measurement on reflector

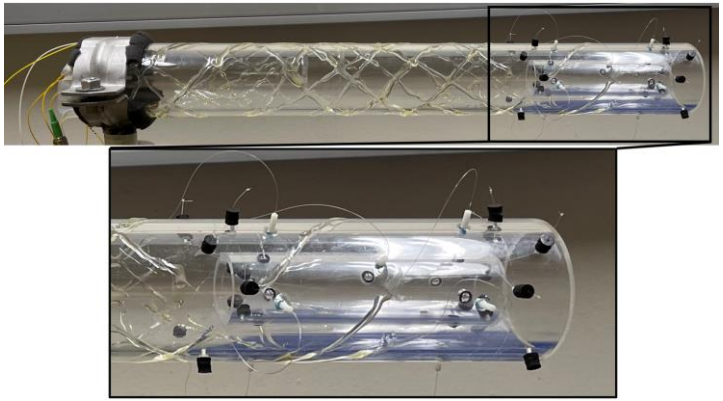

Measurements performed by a single fiber fiber

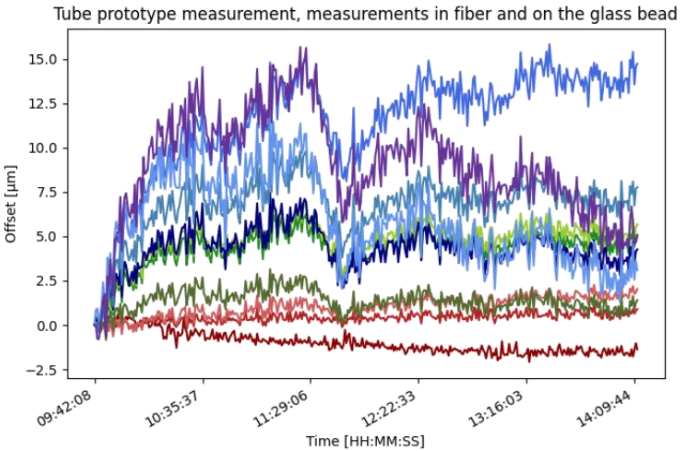

Ongoing ½ scale prototype being built

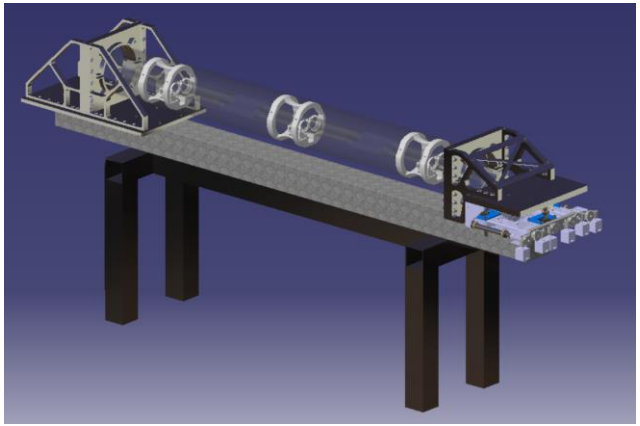

Recovering the data from the fibers

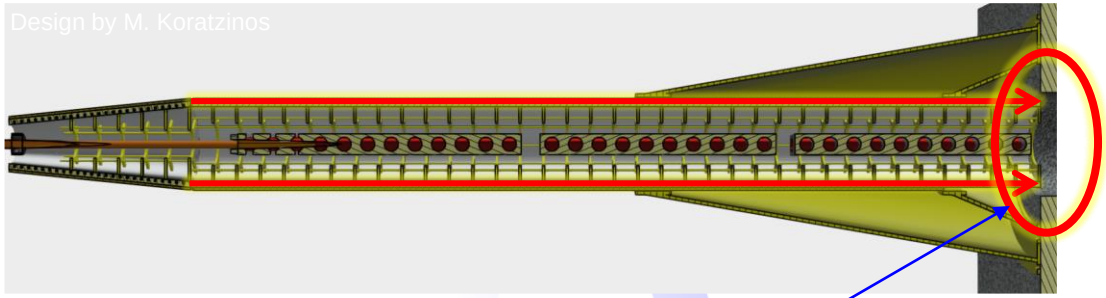

All the information from the fibers will go through there.
Challenges due to conditions (space, temperature gradient, radiations, vacuum …) -> interface with fibers brazed or glued using epoxy.

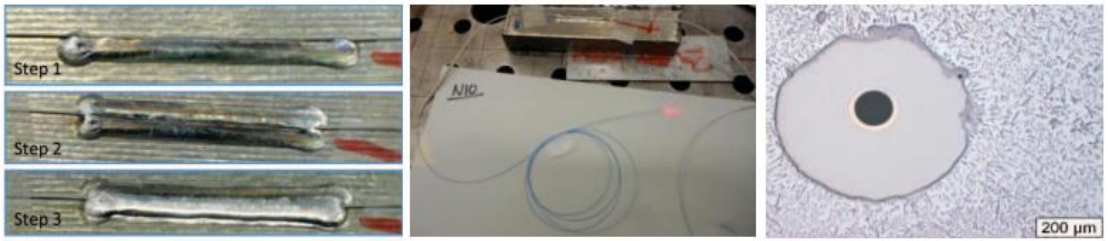

(a) (b) (c)

Figure 2. (a) Optimized 3-step embedding technique with laser brazing, (b) setup with red light fault detector for coarse tuning of the embedding technique and (c) cross section cut of the embedded optical fiber in metal using laser brazing.

Grandal, Tania, et al. "Laser brazing metallic embedding technique for fiber optic sensors." 2017 25th Optical Fiber Sensors Conference (OFS). IEEE, 2017.

Epoxy glued optical fiber for installation on low-beta quadrupole cryostat for HL-LHC

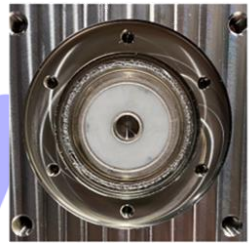

(a) Ceramic washer brazed into the EO-BPM body

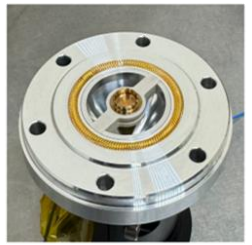

(b) EO-BPM button assembly, mating view

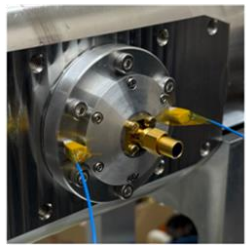

(c) EO-BPM button assembled onto the body

Figure 3: Photos showing detail of the ceramic washer brazed to the EO-BPM body, mating interface to the button assembly and button assembled onto the body.

Bosman, M. Z. C., et al. "DESIGN AND DEPLOYMENT OF AN IN-VACUUM ELECTRO-OPTIC BPM AT THE CERN SPS."

External alignment system

External alignment system proposition

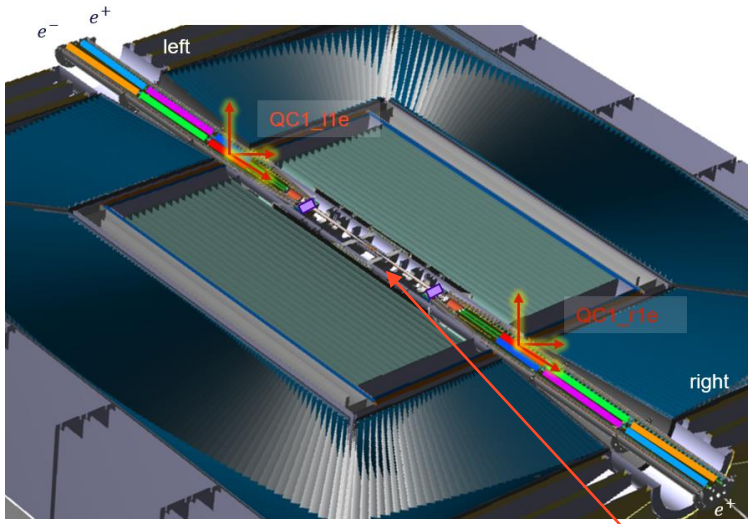

FCC-ee MDI external alignment monitoring system

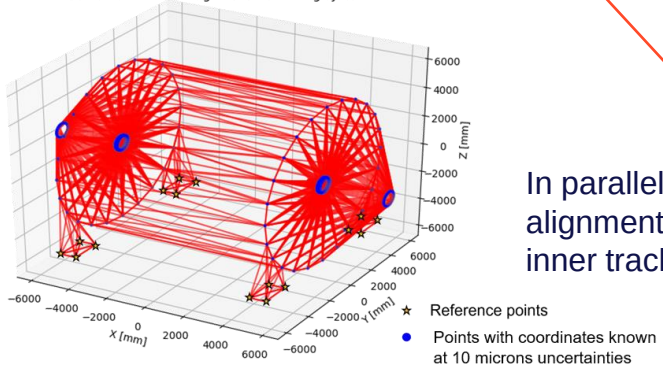

In parallel, currently looking at an alignment monitoring system for the inner tracker

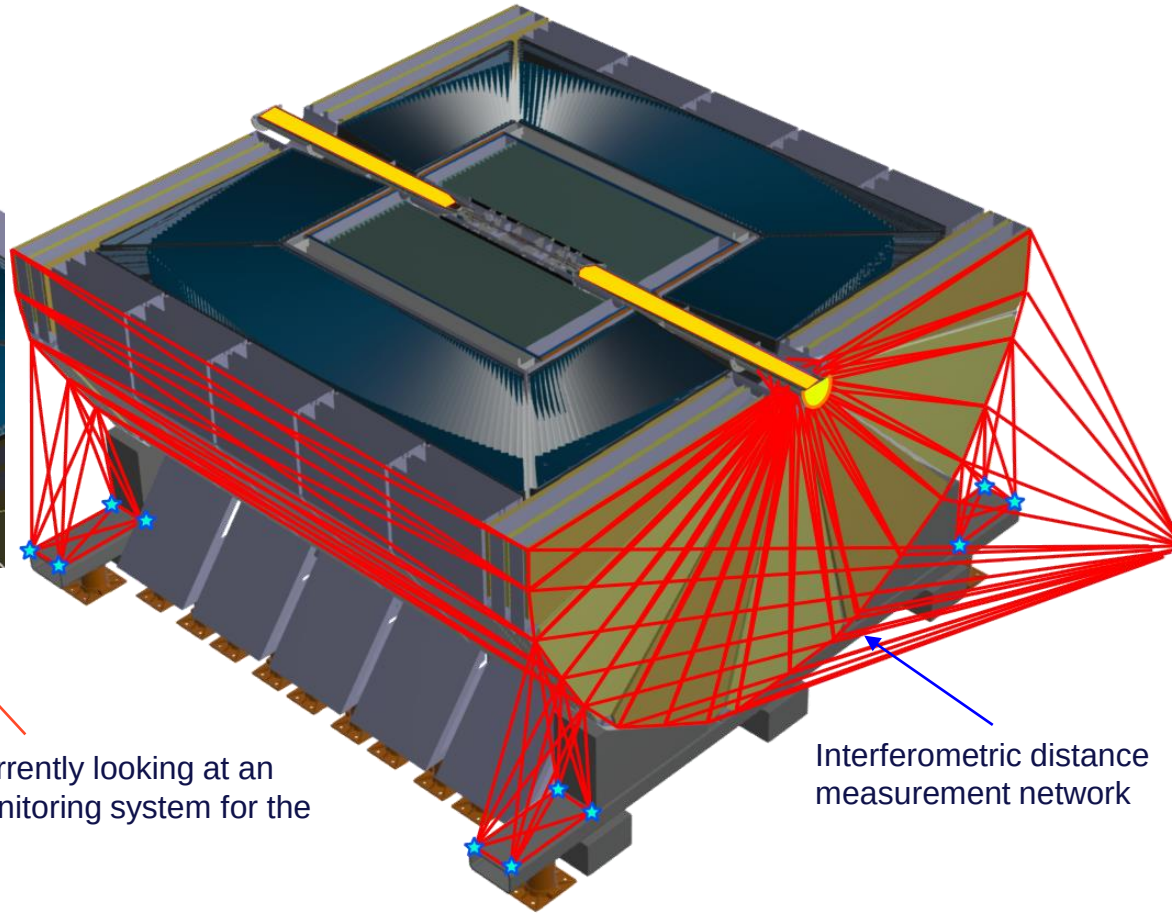

Interferometric distance measurement network

External alignment system sensors

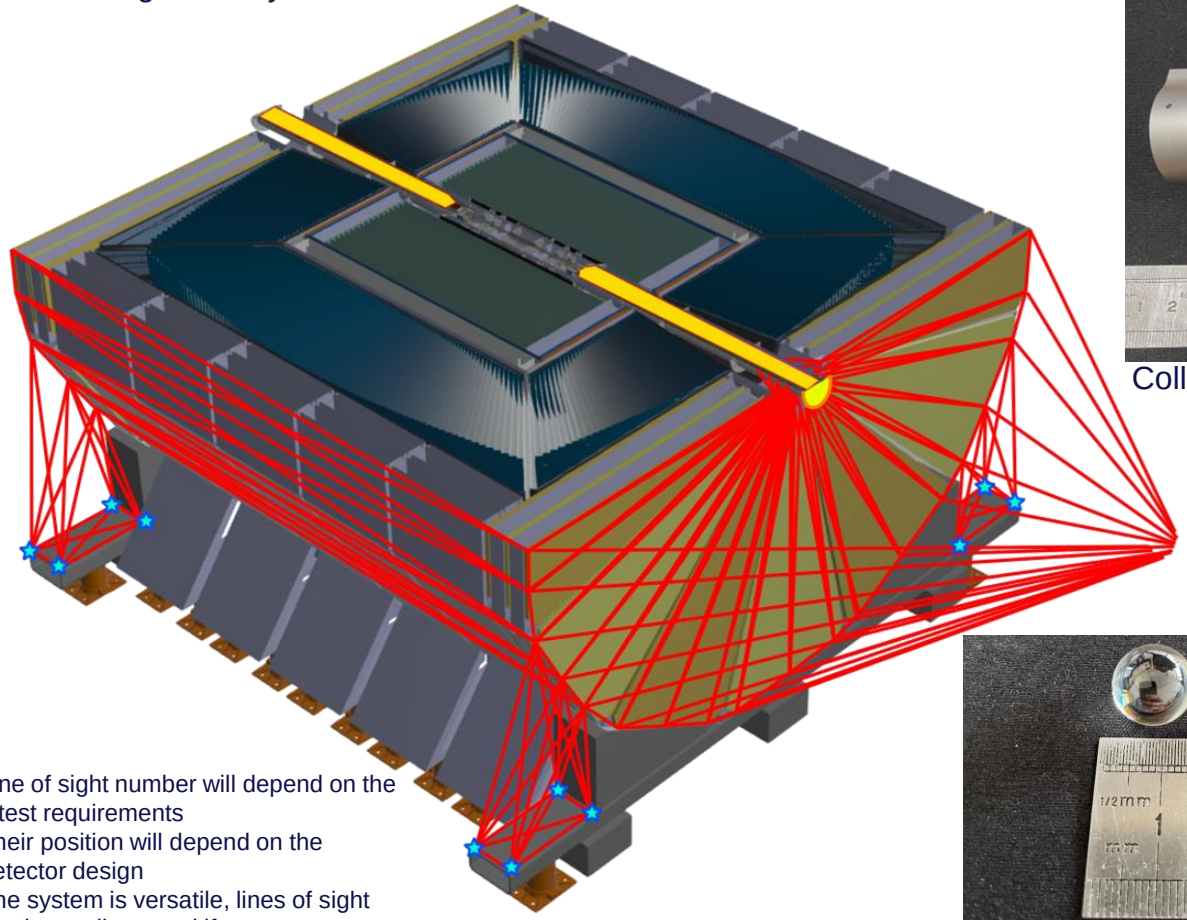

Line of sight number will depend on the latest requirements
Their position will depend on the detector design
The system is versatile, lines of sight can be easily moved if necessary

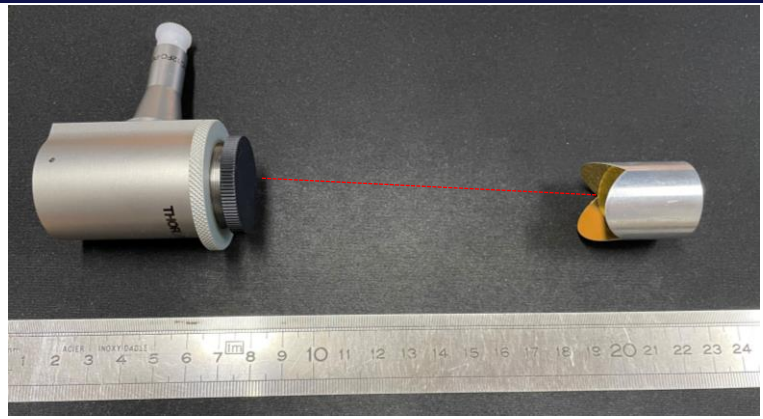

Collimator and Corner Cube retroreflector

Glass bead supports

Glass beads

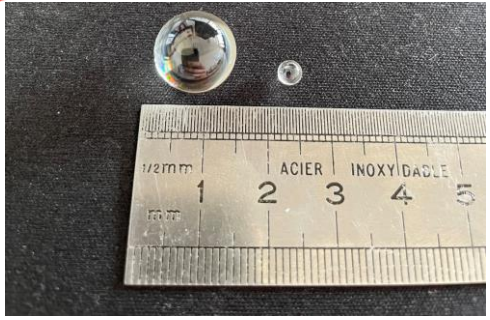

To put to perspective : subdetector monitoring systems installed inside ATLAS

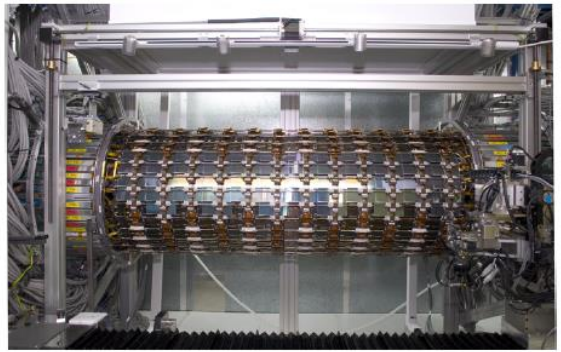

Figure 2: *The smallest barrel of the ATLAS SemiConductor Tracker. Silicon detector modules are robotically mounted onto the Ø 560 mm, 1.5m long carbon-fibre support cylinder.*

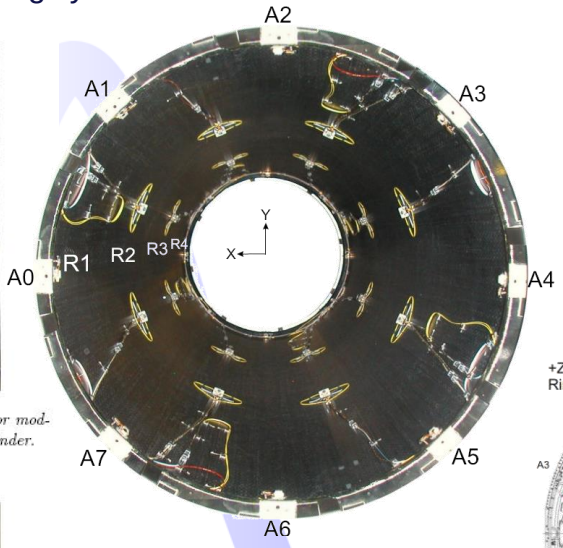

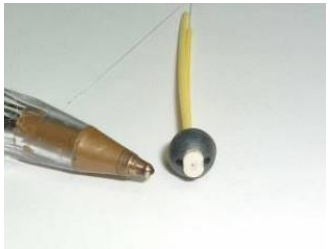

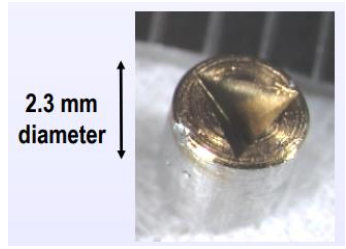

Cf. presentation

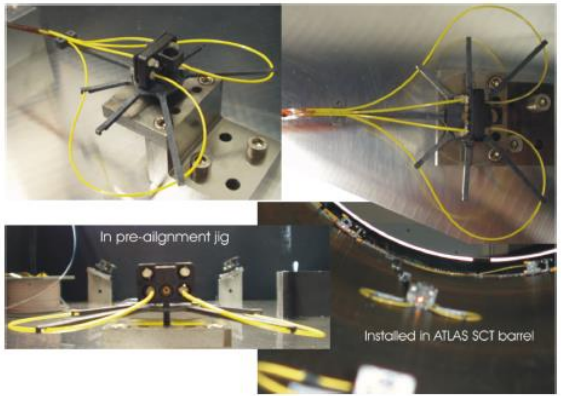

Figure 3: *An ATLAS FSI jewel, called a 'scorpion', is pre-aligned in a jig that replicates the layout of the ATLAS SCT barrel.*

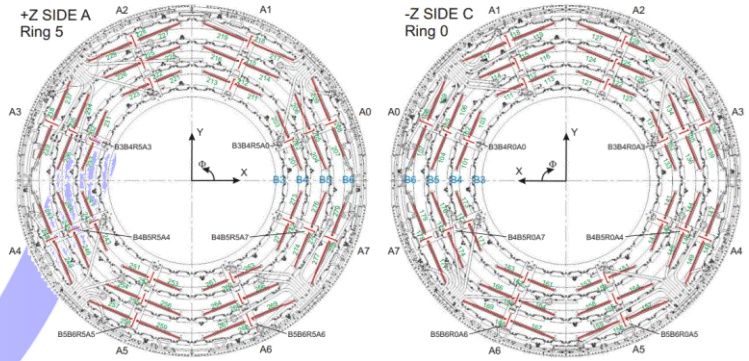

Figure 1: Grid line Interferometer layout on SCT Barrel flanges.

Gibson, S. M., et al. "Monitoring the heart of ATLAS using Frequency Scanning Interferometry." *Proceedings of the Eighth International Workshop on Accelerator Alignment, CERN, Geneva*. 2004.

To put to perspective : subdetector monitoring systems installed inside ATLAS

Example of movement justifying a monitoring system

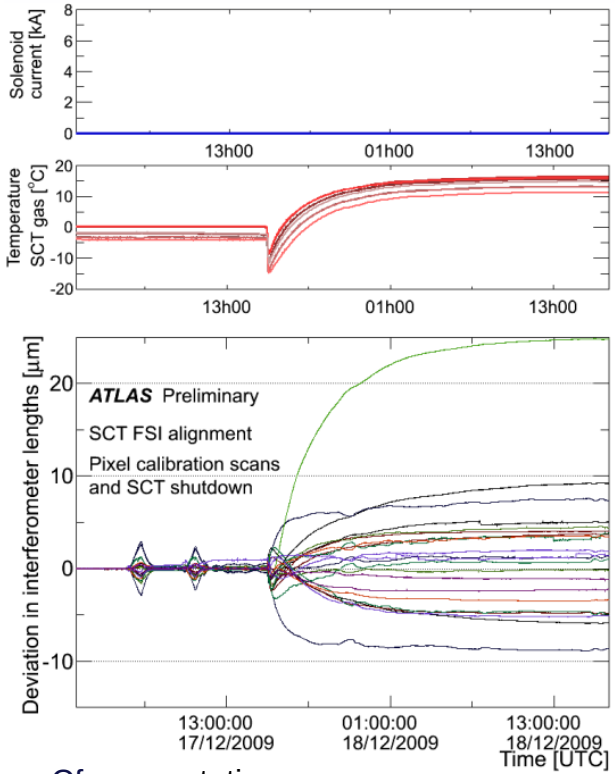

Cf. presentation

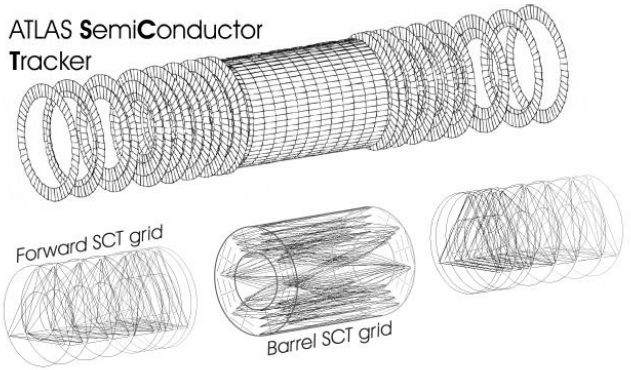

Figure 1: *The layout of the silicon detector modules in the ATLAS SemiConductor Tracker. The three SCT sections are monitored using FSI geodetic grids. Each of the 842 lines represents an interferometric distance measurement between grid nodes. The SCT is 5.6m long.*

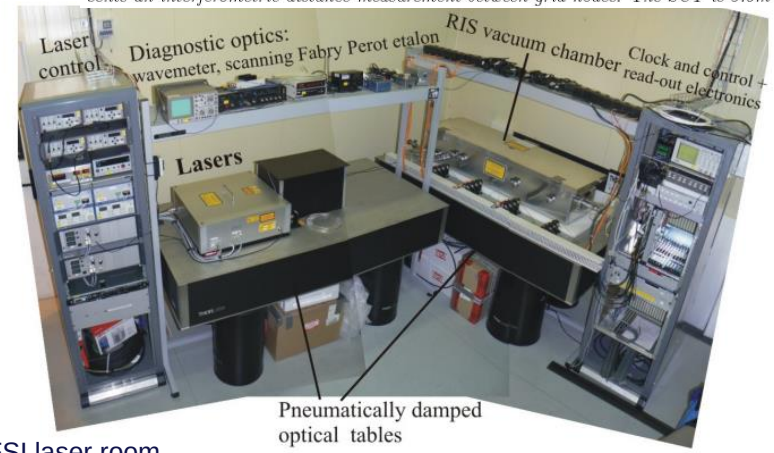

FSI laser room

Gibson, S. M., et al. "First Data from the ATLAS Inner Detector FSI alignment system." *proc. The 10th International Workshop on Accelerator Alignment, KEK, Tsukuba*. 2008.

To put to perspective : subdetector monitoring systems installed inside ATLAS

device class	type	physical	logical	function
in-plane	RASNIK	1984	1984	MDT deformation
MDT temperature	TEMP	96	768	MDT expansion
in-bar	RASNIK	176	352	bar deformation
bar temperature	TEMP		608	bar expansion
radial	BCAM	96	256	bar deformation
polar	BCAM	208	1856	bar-bar link
azimuthal	BCAM	736	1472	bar-bar link
proximity	RASNIK	2384	1192	MDT-bar and MDT-MDT link
laser source	BCAM	584	2208	MDT-bar link
3D sensor	BCAM	192	384	CSC-bar and CSC-CSC link
CSC temperature	TEMP	16	96	CSC electronics monitoring
total		**6648**	**11176**	

Table 3: Classes of alignment devices in the endcap system (temperature sensors on MDT chambers other than the Small Wheel and EML1/EMS1 ones are not read out by the LW-DAQ system and have been omitted). The "physical devices" column lists the number of LWDAQ devices; the "logical devices" column lists the number of acquired sensor images or temperatures, respectively. The device classes and their functions are described in section 3.

Lines of sight

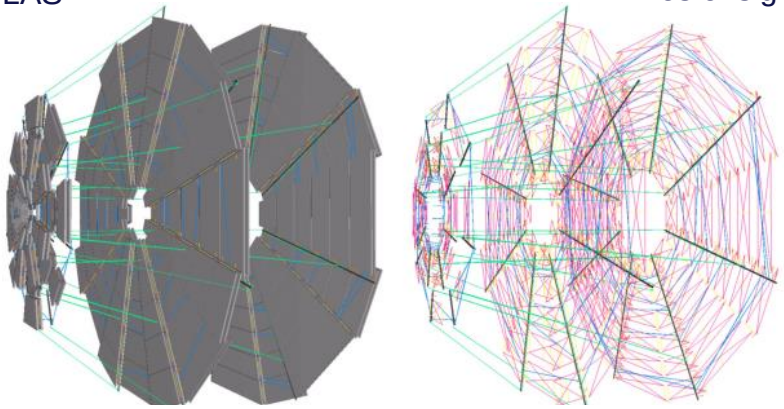

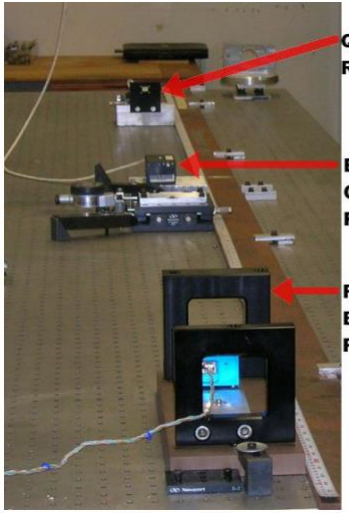

BCAM

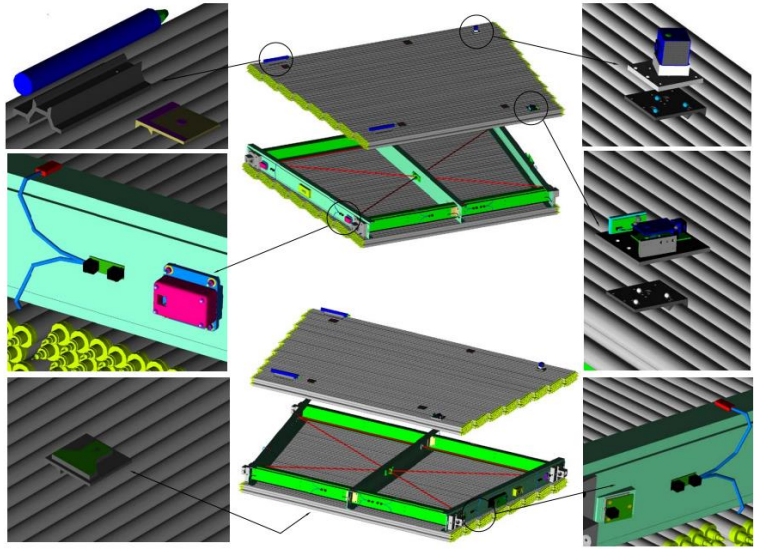

Amelung, Christoph, et al. "The Optical Alignment System of the ATLAS Muon Spectrometer Endcaps." *ATL-MUON-PUB-2008-003* (2008).

External alignment perspectives

Could be interesting to link the alignment with the alignments systems of the subdetectors.

Win/win situation as it would densify the alignment network, making it more robust while also giving precious information of subdetectors relative positions. It will give also the information on the position before the start of the collider, speeding up the initialization.

This link could be also very helpful for assembly and opening procedures, providing a continuous monitoring and validating the position.

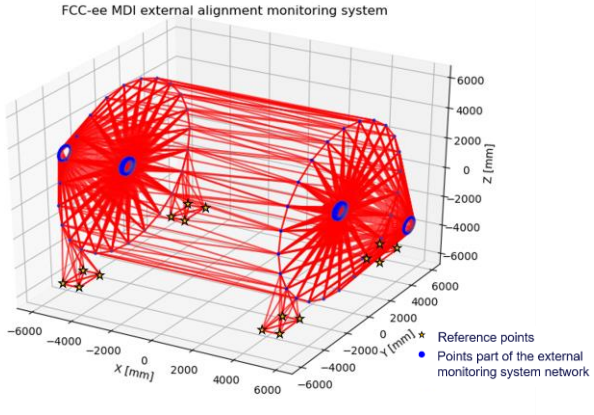

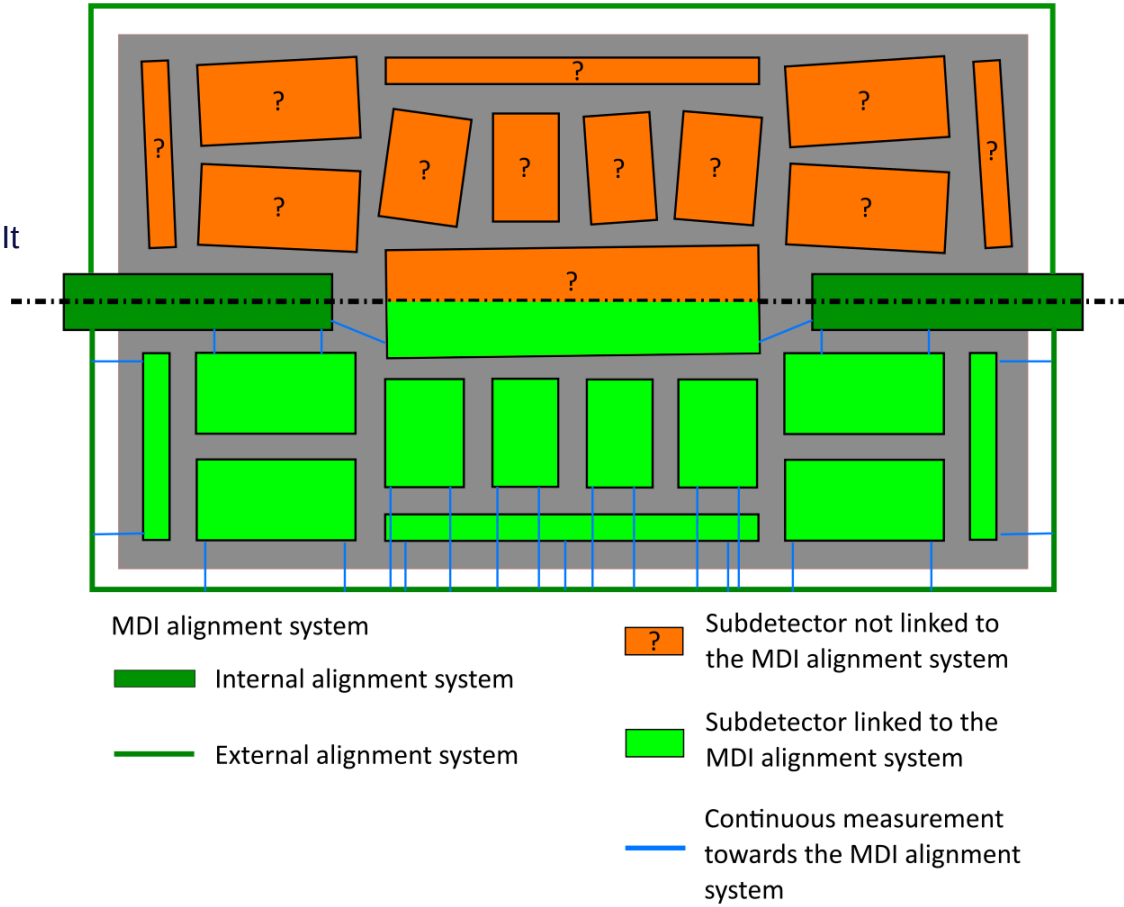

Thank you for your attention

Deformation monitoring

https://iopscience.iop.org/article/10.1088/1361-6501/acc6e3

Cylinder deformations

Helixes observations
(= 3D lengths of portions)

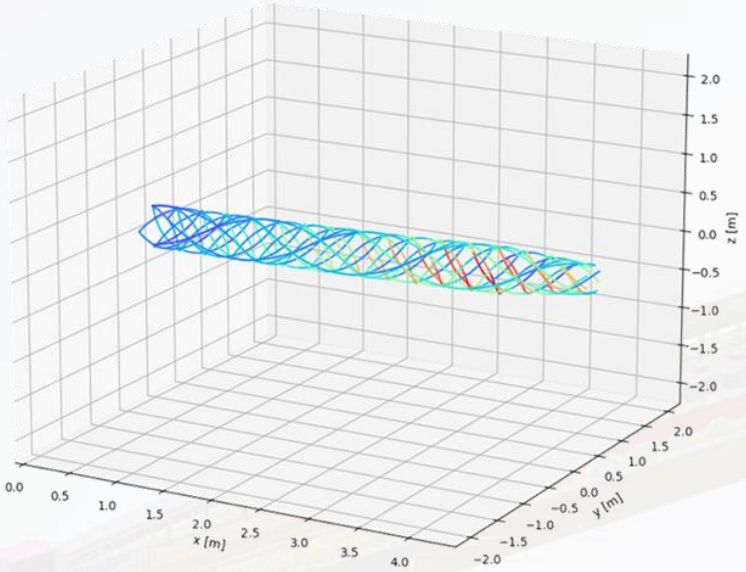

+ equation of portion length as function of the deformation polynomials

Total : 3600 measurements and ≈ 3 cm³ space taken by the sensing system in the assembly.

Least square adjustment

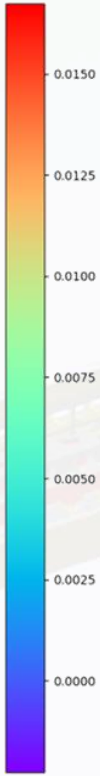

$$P_x(t) = \sum_{i=1}^{n} a_i t^i$$
$$P_y(t) = \sum_{i=1}^{n} b_i t^i$$
$$P_z(t) = \sum_{i=1}^{n} c_i t^i$$
$$P_\theta(t) = \sum_{i=1}^{n} d_i t^i$$
$$P_{ry}(t) = \sum_{i=1}^{n} e_i t^i$$
$$P_{rz}(t) = \sum_{i=1}^{n} f_i t^i$$

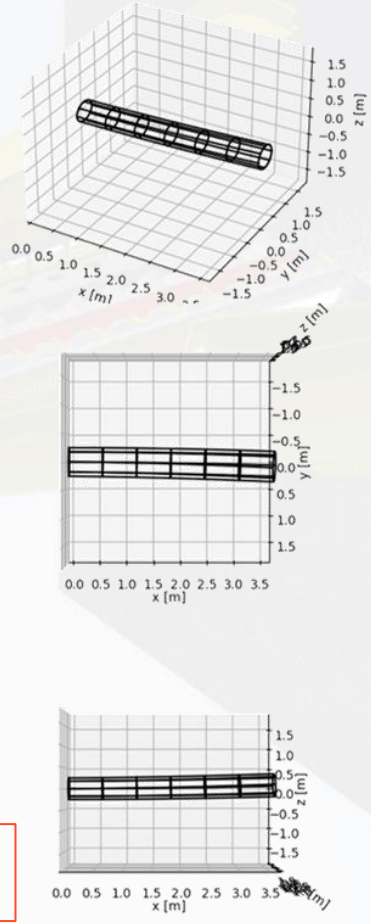

Simulations shown micrometric accuracy
To be confirmed by a prototype

More info on the FSI monitoring of the SCT in ATLAS

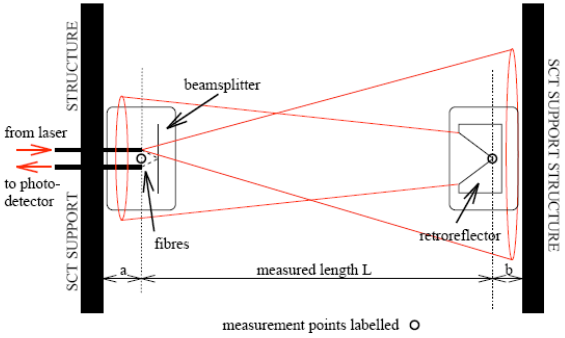

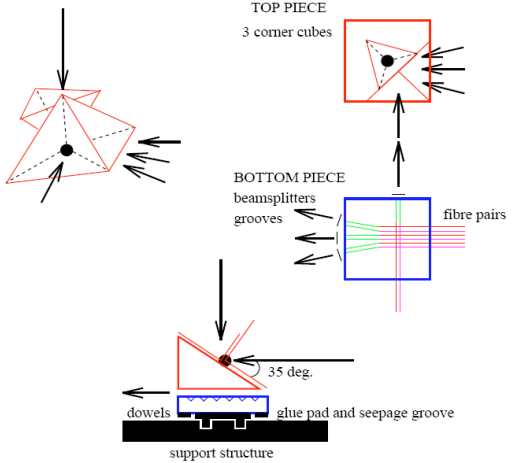

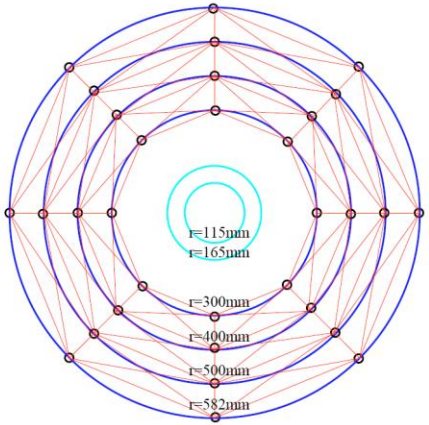

Figure 7: *A possible alignment grid for the end-planes of the Si barrel. It is expected that there will be a thin plane in which the required lines of sight are available. There are 64 variables to be determined (r and φ for 32 points), and 104 measurements (13 per octant).*

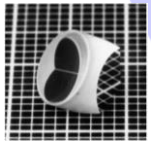

Fox-Murphy, A. F., et al. "Frequency scanned interferometry (FSI): the basis of a survey system for ATLAS using fast automated remote interferometry." Nuclear Instruments and Methods in Physics Research Section A: Accelerators, Spectrometers, Detectors and Associated Equipment 383.1 (1996): 229-237.

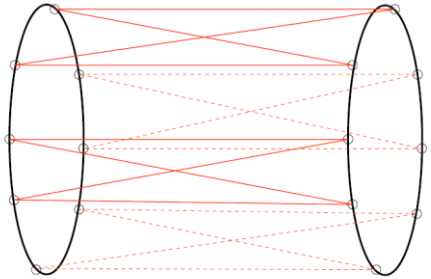

Figure 8: *A possible longitudinal alignment grid. These measurements would ideally be made for each of the 4 cylinders giving 64 measurements in total. An additional plane of measurements may be inserted between the end-planes.*

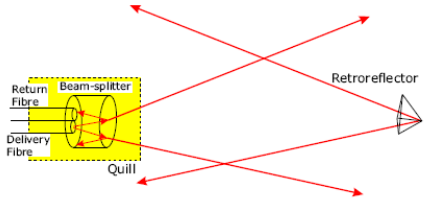

Figure 1.16: *The design of a grid line interferometer to be installed in the ATLAS SCT. N.B. The sizes of the quill and retroreflector shown here are both exaggerated.*

Coe, Paul Andrew. *An Investigation of Frequency Scanning Interferometry for the alignment of the ATLAS semiconductor tracker*. Diss. University of Oxford, 2001.

Summary of the FCC-ee MDI design